Suplemento de la Revista Mexicana de Física **1** (2) 45–50 JUNE–JULY 2020

Experimental study of capillary penetration in rectangular Hele-Shaw cells closed by two edges

R. Diez Barroso-Agraz and G. Gómez-López
Instituto Politécnico Nacional, SEPI ESIME Zacatenco,
Av. Miguel Othon de Mendizabal SN, La Escalera, Ciudad de Mexico.
e-mail: ronier.diezb@gmail.com; laguerre.legendre@gmail.com

A. López-Villa
Instituto Politécnico Nacional, SEPI ESIME Azcapotzalco,
Calz. Azcapotzalco - La Villa, El Jaguey, Azcapotzalco, Ciudad de Mexico.

D.A. Serrano
Facultad de Ciencias, Universidad Nacional Autónoma de México,
Exterior Circuit S/N, C.U., Coyoacán, 04510 Ciudad de Mexico.
e-mail: arman2390@hotmail.com

Received 19 de febrero de 2020; accepted 27 de marzo de 2020

Here we study the capillary penetration of a viscous liquid between two vertical, rectangular close together plates. In the experiments, the plates were joined simultaneously along two edges, and the liquid penetrated from the bottom. Spacers with different geometries like circular, triangular and rectangular shape, were used to study their effects on the rise profiles in a dynamic way, it was noticed that when time evolves, the profiles are stabilized in a catenary and the instabilities induced by efforts present in the plates disappear. It was also observed that the rate of ascent differs from the classical values of $t^{1/3}$ or $t^{1/2}$, depending on the effect of gravity.

Keywords: Surface tension and related phenomena; liquid thin films; liquid thin film structure: measurements and simulations.

PACS: 68.03.Cd; 68.15.+e; 68.18.Fg

1. Introduction

In nature, there are many biological and natural systems that inspire the development of different technologies, one of these systems is the transport of liquids on surfaces with characteristic hierarchical structures, *i.e*, surfaces that address the water transport of other fluids, one of most studied cases is the water transport in plants, in particular through xylem of trees, achieving its transport from the subsoil up to a height of over 100 meters. Other case is the study of the prey-trapping pitcher organs of the carnivorous plant Nepenthes alata. It was found [6] that continuous, directional water transport occurs on the surface of the 'peristome' in the rim of the pitcher due to its multiscale structure, which optimizes and enhances capillary rise in the transport direction, and prevents backflow by pinning in place any waterfront that is moving in the reverse direction. It results not only in unidirectional flow, despite the absence of any surface-energy gradient, but also in a transport speed that is much higher than previously thought [6], in this article, it has been studied similar topics like-named "Surfaces Inspired by the Nepenthes Peristome for Unidirectional Liquid Transport".

As background of works previously mentioned that take the first steps towards this path, *i.e*, studies about capillary ascent initially studied experimentally by Taylor [2] and Hauksbee [3], three centuries ago to show the existence of the capillary driven force as well as the formation of equilibrium profiles. In both works, is reported that equilibrium profiles were rectangular hyperbolas with a very important peculiarity; near the edge, liquid tends to reach an infinite height, which in nature is very suitable to supply water and sap (which contains the nutrients) to the upper leaves of tall trees as mentioned before, subsequently, studies of the capillary ascent between two plates joined by an edge were formed a small angle (wedge) as in the case of Finn and Concus in 1969 [10] and in 1993 adding cylindrical coordinates [11] and subsequently studied by Ponomarenko [4] who proposed a power law of fluid ascend of $t^{1/3}$ trying to find a universal law, in 2008 is retaken by Medina and Higuera, where a

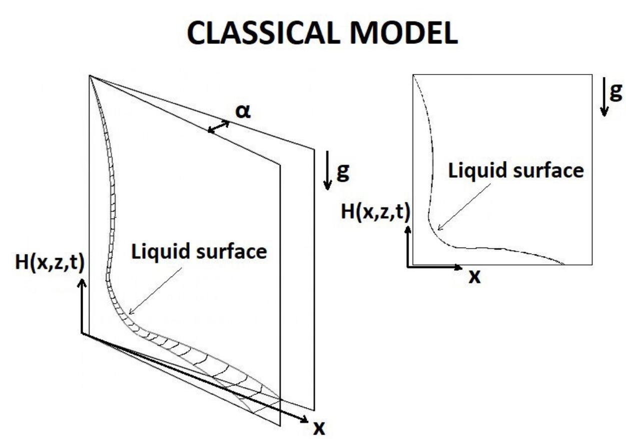

FIGURE 1. Classic model of hele-shaw cells used by Taylor [2] , Ponomarenko [4] and Higuera [5].

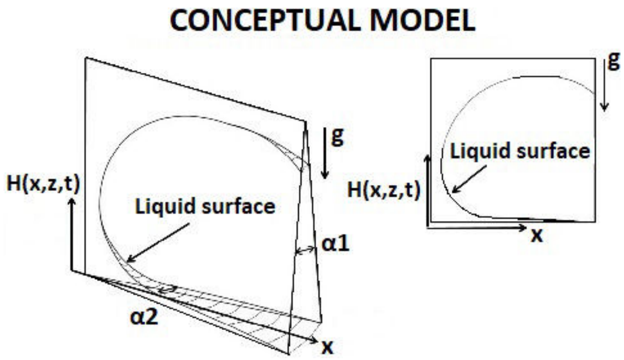

FIGURE 2. New model proposed.

model is developed which is already a classic due to the amount of studies that have been made with it, see Fig. 1.

In this last work the dynamic of capillary ascent is studied, which had not been described since the first studies, and where a velocity of ascent appears once again of $t^{1/3}$, all of these works are important due to the fact that if humans can understand the operation of bio-inspired and biomimetics media, it will be easier to understand primordial processes in human development, for example, mechanical devices like cooling, adsorption, condensation and medical applications like blood irrigation, to mention some.

For our case, this work has been based in the classical design of Hele-Shaw cells but adding two new conditions, one of these are performing another union in the upper side of cells (Fig. 2), bringing about two aperture angles named $\alpha 1$ and $\alpha 2$ that produce a complex geometry for study, this proposal is based in the model of Chen and Zhang *et al* [6] and the developed work presented by Yu Tian *et al*. [7] , the second condition was the geometry of the spacer like the case of the second experiment presented by Géraud *et al* [8], for this case the spacers used were of circular, square and triangular geometries (for the triangular spacer case no graphics are shown, this is due to the fact that fluid displacement time is very long).

The development of this work is essential for the creation of a dynamical model of capillary ascent in wedges with complex geometries at different opening angles; this can be considered as an idealization of a fracture of a real rock as in other previous works, however, the difference between this work and previous developments lies in the displacement of the fluid not only by one of its edges but by two edges see Fig. 2.

2. Experimental Procedure

For the development of the experiments two acrylic plates of three millimeters thickness were used, these plates were joined by one of their sides and on the upper side and their walls were separated from each other with different kind of objects with circular and square geometries, achieving openings from 3.5 to 9 mm, the distance of aperture was measured with a Vernier caliper. The diameter of the circular geometry is 25.5 mm and the measure of the square geometry was considered inscribed in the circumference. In Fig. 2 a graphic experiment representation is shown. A catenary is expected to be obtained that approaches the sides where the plates have been joined, there are opening angles α_1 and α_2 which for this case have the same magnitude, the fluid ascends in direction H which is dependent of time, direction x and direction z.

The experiments were made inside a wooden box with black walls, every wall had 40 cm tall and long and only one of the walls had a white surface see Fig. 4. The black walls avoided reflection generated by light, the white wall allowed to follow the movement of the fluid, this colour contrast made it possible to watch the motion of the fluid concerning for to time. Images of the experiment were taken using a cell cam-

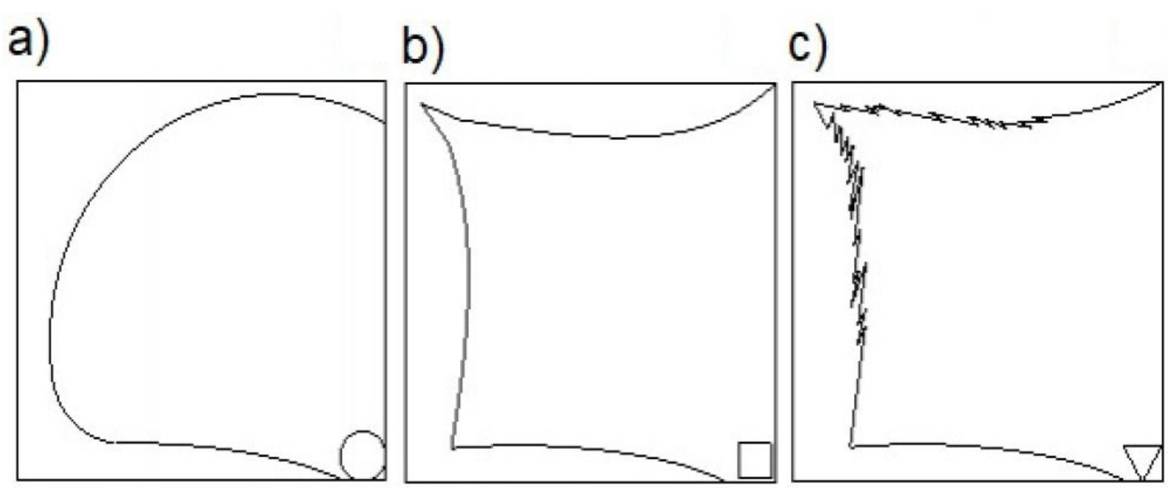

FIGURE 3. Profiles generated with different kind of spacers. a) Profile with circular spacer. b) Profile with square spacer. c) Profile with triangular spacer.

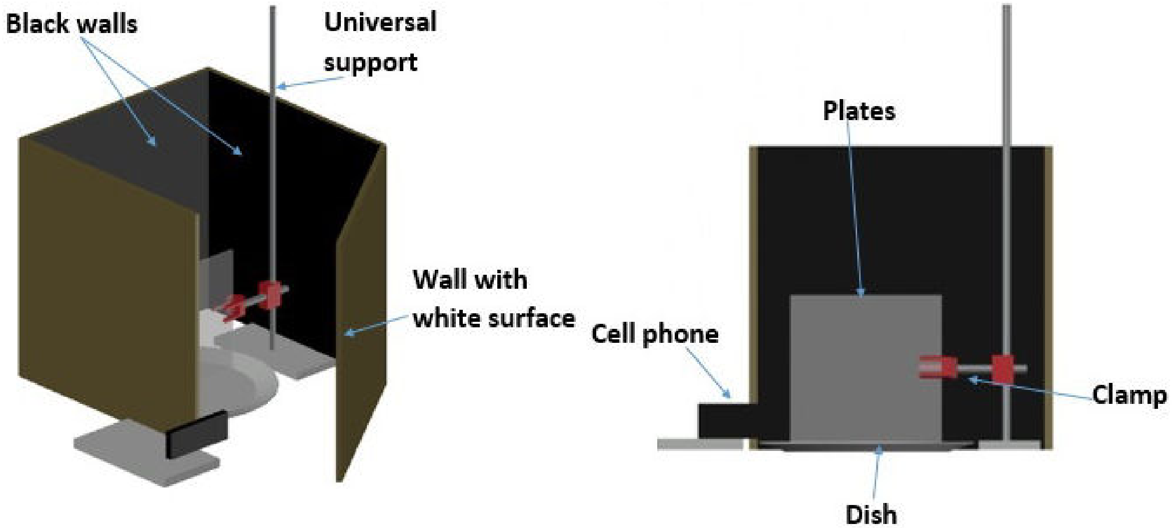

FIGURE 4. Elements used in experiments.

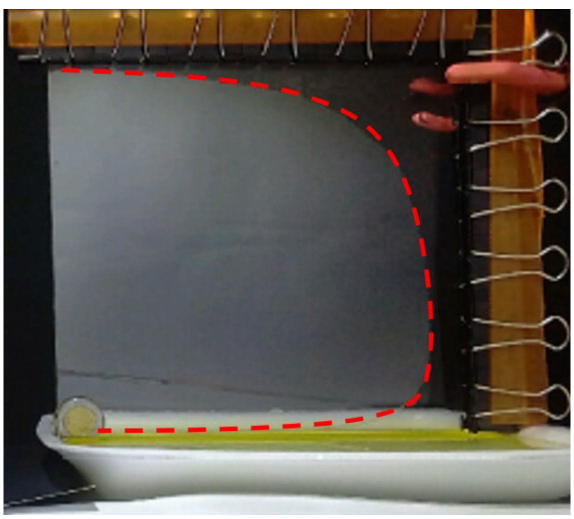

FIGURE 5. Final expected profile.

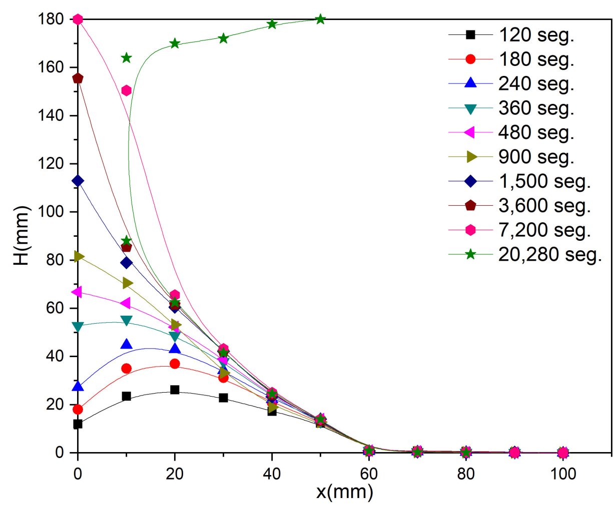

FIGURE 6. Opening angle: 3.08°. Geometry of spacer: circular.

era of 8 megapixels and an app named "infinite shot" that takes pictures in intervals of 60 s, at the end of the experiment the app collected all images and created two files, one of these contained all the images taken by the app, the other file stored a video in .mp4 format. The plates joined by 2 of its sides were placed on top of a dish that contained kitchen oil and those plates were clamped with an universal support.

3. Experimental Results

The final profile expected a large angle of (8.08°) but, in this case, the profile was formed over a long period of time and the shape of the catenary looks symmetrical compared to the graph of its experiment. In the red striped line is possible to see the catenary that represents the final profile of the experiment. This kind of profile is hoped for all the aperture angles using a circular spacer, the difference between them is the time it takes to complete the path or to shape the catenary.

The graph of Fig. 6, shows profiles generated at different times, as can be seen, the obtained profiles follow the kind of growth mentioned by A. Medina and F. Higuera. The considered times have been random and in the graph of green colour it is possible to perceive that the profile when this is ascending, this is thinned in the straight line z. It is necessary to mention that the unit of distance traveled in the experiments will be in millimetres (mm) in this way the phenomenon is better understood.

In the graph of Fig. 7, the same kind of profile growth is shown again. It is possible to notice that a greater angle opening the column H becomes thinner, also besides, the pink profile (final profile) has completed the route between the plates at the same time that the green graph of Fig. 6 which just arrived at 50 mm on the $x-$axis considering the same time.

In this graph of Fig. 8, it is shown that approximately to the 140 mm in $z-$axis (H(mm)) and the 25 mm in $x-$axis

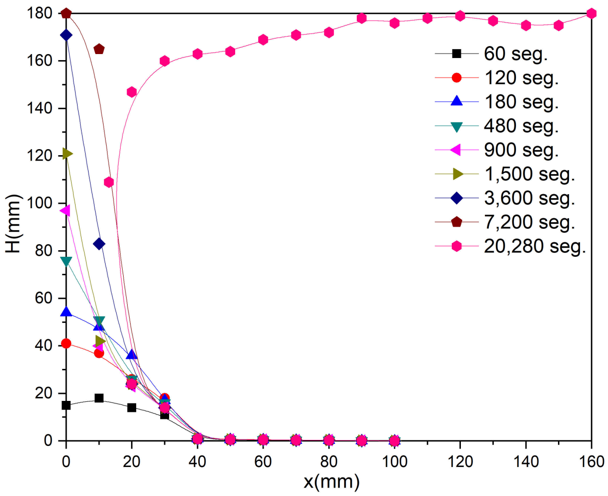

FIGURE 7. Opening angle: $5.08°$. Geometry of spacer: circular.

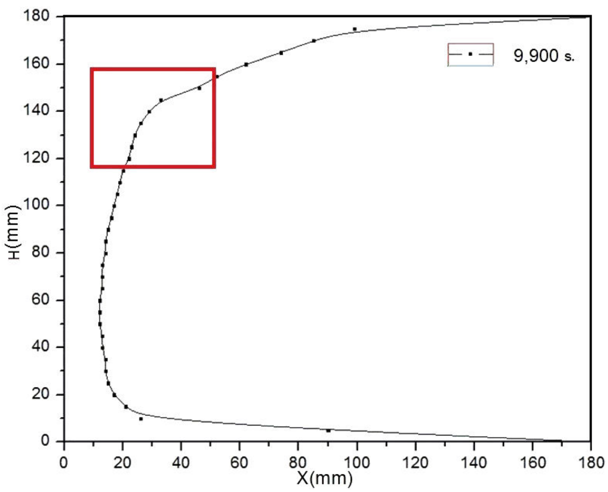

FIGURE 8. Opening angle: $8.08°$. Geometry of spacer: square.

a small perturbation in the catenary is generated (it is possible to see this section inside the red box), this is known as an irregularity produced by the efforts that are generated in the plates opened by a square geometry which points from one of its vertices towards the area where the irregularity occurred, however, this irregularity is hardly noticeable because the aperture angle is too large, in the case of small aperture angles, this irregularity is very easy to see.

As it is mentioned above, at extended times the profile is still changing and tends to an equilibrium profile, in this case, with a square geometry spacer it is perceived that it can reach an equilibrium position of fluid and this is how the minimum energy principle manifests [9,10] , the time of execution must be long and if the aperture angle is greater the irregularities are less than a smaller aperture angle, so in the case of this experiment with a smaller angle, the irregularities in profile are more perceptible than a greater aperture angle.

After 96 hours with a square spacer, the fluid tends to an equilibrium position and it is possible to notice a similar catenary to that of the spacer with a circular shape, but in this case, the period of time of execution is long, however, in both of them, the equilibrium is reached no matter the aperture angle and the aperture geometry.

In the graph of Fig. 11, a comparison is made before an apparent final profile is generated (a final profile is the one that makes a total route between the plates) against the denominated equilibrium profile (because it no longer modifies its position concerning for to time). It is possible to notice that in the black colour graph (equilibrium profile), the fluid has covered a greater area, however, it is possible to notice irregular patterns due to efforts generated by the aperture of a square geometry. The irregularities can be noticed in the intervals between 80-130 of H axis and in the 30-60 of x-axis.

When the plates have a triangular spacer between its walls, the profile generated in picture $a)$ it is possible to notice an incomplete profile after 96 hours of experiment, so that demonstrates that a triangular spacer produces a partial profile over a long period of time while in picture $b)$ the profile has reached an equilibrium position in which it is possible to see again how a circular profile is generated.

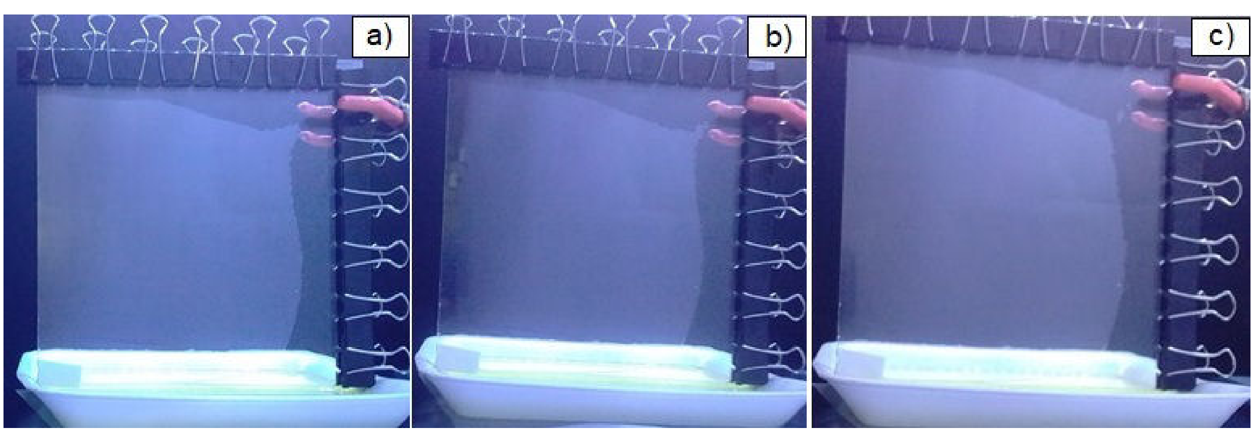

FIGURE 9. Change in the spacer. Opening angle: $3.08°$. Opening geometry: square. a) Profile generated in 24 hours. b) Profile generated in 48 hours. c) Profile generated in 72 hours.

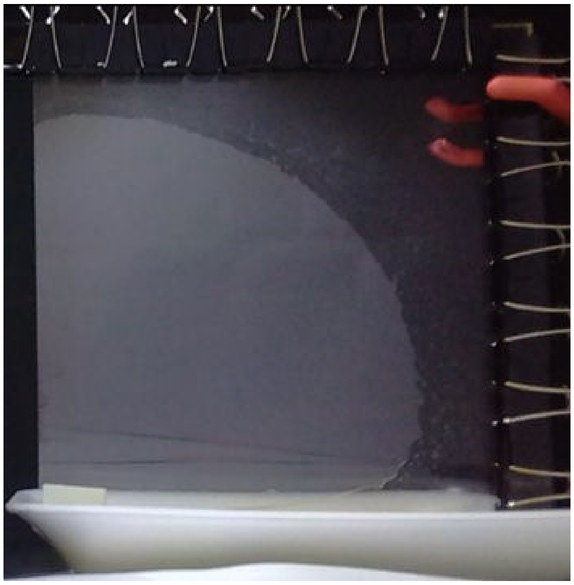

FIGURE 10. Final profile obtained with a square spacer.

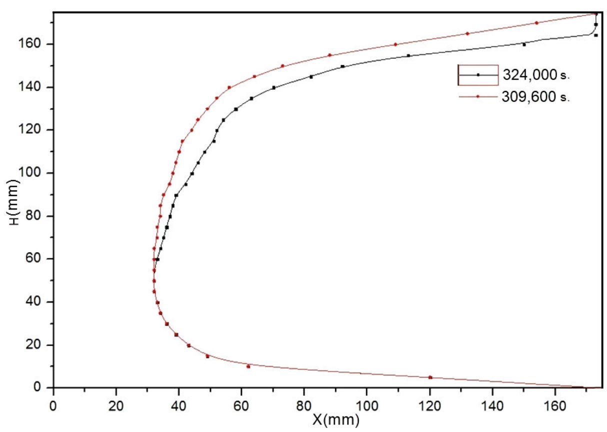

FIGURE 11. Square spacer inserted between plates.

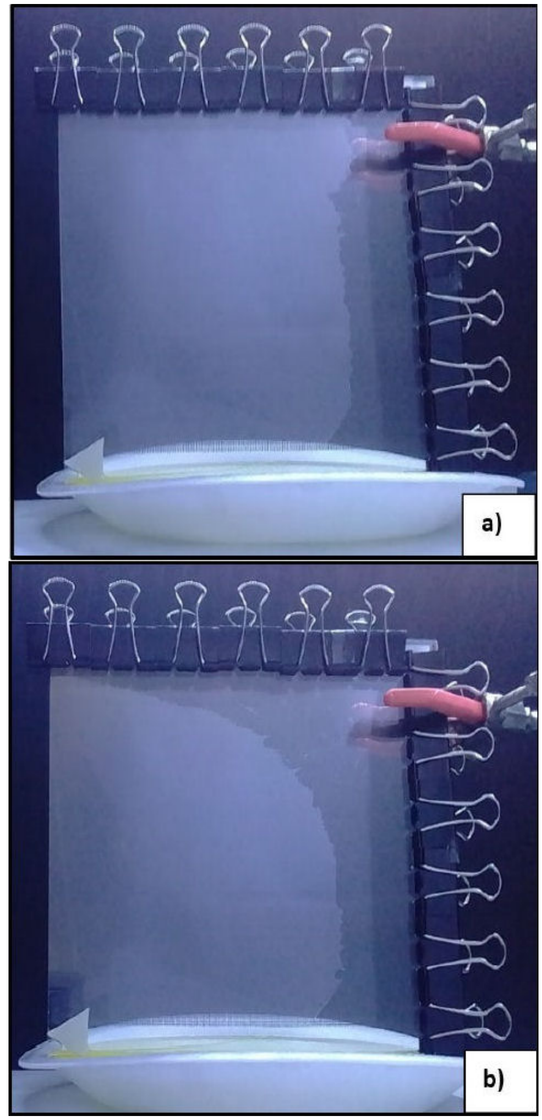

FIGURE 12. Profile generated with triangular spacer. a) Generated profile after 96 hours. b) Generated profile when the fluid is in a equilibrium position.

4. Conclusions

As the aperture angle decreases, the time taken to complete the profile increases, this can be firstly corroborated in the cases of experiments with the circular geometry spacer, in the case of an aperture angle of 5.08° its time path of profile was of 20,280 s while in the case of aperture angle of 3.08° it can't complete its path at the same time, this can be justified by the space that the fluid must fill, when this space is very small the fluid must to fill a greater quantity of bulk.

The geometry of the object that opens the cells is also involved in the time of profile path, this can be corroborated in the case of square spacer in comparison with the cases of circular spacer. While in experiments with a circular aperture angle the time path of profile was of 86,400 s (maximum time), in the situation where the geometry of aperture was a square, the time path was of 309,600 s (even though its aperture angle was large) but this was an apparent formed profile as we let time pass, the profile continues to go down and to fill the space, reaching its final profile in a time of 324,000 s.

When exist a square geometry of spacer, it delayed about 16 times more than major aperture angle with circular geometry, but in case of the square spacer with 3.08° of aperture angle was decremented, the time path it increases until 96 hours, so it is totally verifiable that the opening angle and the geometry of the opening object are related to the time in which the profile is formed.

As can be seen in a square spacer with 3.08° of aperture angle, when a long period of time is considered regardless of the geometry of the opening, the profile always becomes a catenary and this is a perceptible principle in nature since all bodies will tends to a position of equilibrium and this generates a curve, this has been called the minimum energy principle.

Acknowledgments

To Consejo Nacional de Ciencia y Tecnología (CONACyT) for the financial support granted during the masters degree in thermofluid sciences. To Instituto Politécnico Nacional and the Sección de Estudios de Posgrado e Investigación for allowing me to use its resources and facilities and for providing the necessary support to carry out this project.

1. A. Jara, S. De Santiago, F. J. Higuera, M. Pliego, A. Medina, and C. A. Vargas, *Capillary rise in a Taylor-Hauksbee cell with a tilted edge*. In Selected Topics of Computational and Experimental Fluid Mechanics (pp. 541-548). (Springer, Cham. 2015).
2. B.Taylor, *Philos*, **27** 539.
3. L. F. Hauksbee, *Philos. Trans. Royal Society. London* **27** 539.
4. A. Ponomarenko, D. Quéré, and C. Clanet, *J. Fluid Mech*. **666** (2011) 146.
5. F. Higuera, A. Medina, and A. Liñan, *Physics of Fluids* **20** (2008) 102102.
6. H. A. Chen *et al.*, *Nature* **532** (2016) 85.
7. AJ. Z. M. D. Yu Tian, Ying Jiang, *Langmuir* (2019) 5183.
8. S. B. Géraud, L. Járgensen, L. Petit, H. Delanoe-Ayari, P. Jop, and C. Barentin, *EPL (Europhysics Letters)*, **107** (2014) 58002.
9. J. Tielking and W. Feng, "*The application of the minimum potential energy principle to nonlinear axisymmetric membrane problems*", (1974).
10. A. Bhattacharjee and R. L. Dewar, *Phys. Fluids* **25** (1982) 887.
11. P. Concus and R. Finn, *Proceedings of the National Academy of Sciences of the United States of America*, **63** (1969) 292.
12. P. Concus and R. Finn, "*Capillary surfaces in a wedge: Different contact angles*" (1993).
13. S. de Santiago Aguilar, *El problema de taylor inclinado*, Master's thesis, Escuela Superior de Ingenierá Mecánica y Eléctrica, (Instituto Politécnico Nacional, 2015).
14. B. Hamrock, *Fundamentals of fluid film lubrication*. McGraw-Hill series in mechanical engineering, (McGraw-Hill Higher Education, 1994).
15. U. Bauer, H. F. Bohn, and W. Federle, *Proceedings of the Royal Society B: Biological Sciences* **275** (2007) 259.
16. Y. Di, X. Xu, and M. Doi, *EPL (Europhysics Letters)* **113** (2016) 36001.
17. H. Chen, L. Zhang, P. Zhang, D. Zhang, Z. Han, and L. Jiang, *Small* **13** (2017) 1601676.
18. P. Zhang, L. Zhang, H. Chen, Z. Dong, and D. Zhang, *Advanced Materials* **29** (2017) 1702995.
19. E. W. Washburn, *Phys. Rev.* **17** (1921) 273.
20. T. Cambau, J. Bico, and E. Reyssat, *EPL (Europhysics Letters)* **96** (2011) 24001.